

# Optimal photon pairs for quantum communication protocols

M. Lasota\* and P. Kolenderski

*Faculty of Physics, Astronomy and Informatics, Nicolaus Copernicus University, Grudziadzka 5, 87-100 Toruń, Poland*

(Dated: December 21, 2024)

We theoretically investigate the problem of finding optimal characteristics of photon pairs, produced in the spontaneous parametric down-conversion (SPDC) process, for fiber-based quantum communication (QC) protocols. By using the accessible setup parameters, the pump pulse duration and the extended phase-matching function width, we minimize the temporal width of SPDC photons within the general scenario. This allows one to perform more effectively the temporal filtering procedure, which aims at reducing the noise acquired by the measurement devices. Moreover, we compare the obtained results with the achievable parameter values for SPDC sources based on  $\beta$ -Barium Borate (BBO) crystal. We also investigate the influence of non-zero detection timing jitter. Finally, we apply our optimization strategy to a simple quantum key distribution scheme to show that the full optimization of an SPDC source can potentially extend the maximal security distance by several tens of kilometres, which is around 50% more as compared to previous approaches.

## I. INTRODUCTION

Quantum communication is a vast field of physical science focused on improving the process of information distribution among spatially separated entities with the use of quantum mechanics. The exploration of various types of quantum correlation and application of fundamental quantum laws has led to a plethora of proposals for novel communication protocols, including quantum key distribution [1, 2], secret sharing [3], quantum teleportation [4], quantum repeaters [5] and dense coding [6]. However, the initially proposed theoretical versions of these protocols have typically assumed ideal performance of the setup elements required for their physical realization, which is unreachable in practice. As a consequence, the performance of real-life implementations of QC protocols has been severely limited.

Realization of many such schemes requires using sources of single photons or entangled photon pairs. One of the most popular types of them are the devices utilizing the phenomenon of spontaneous parametric down-conversion [7, 8]. It is a process in which a single photon, travelling through a nonlinear crystal, decays into a pair of lower-frequency photons that are typically entangled in many degrees of freedom. Such a source can also be used as a single-photon source, in which case generation of a particular photon is heralded by the detection of another photon from a given pair. SPDC sources have many advantages, including high quality of the emitted photons [9–11], high generation and collection efficiency [12–15] and relatively low cost of their construction. Therefore, they have been extensively used in practical implementations of many QC protocols [16–22].

However, the photons born in the SPDC process are not monochromatic. Instead, they are described by a probability density amplitude distribution, which in most cases can be conveniently approximated by a two-dimensional Gaussian function [23, 24]. These photons

propagate through dispersive media with wavelength-dependent velocity. As a consequence, the longer their travelling distance is, the larger is the uncertainty of their exact arrival times at the destination point. This means that the temporal width of these photons, defined as the standard deviation of the probability distribution function for the time of their arrival, grows with the length of the utilized dispersive quantum channel.

The issue described above can be a major drawback for long-distance QC schemes using typical telecommunication fibers. The reason for this stems from the fact that one of the main factors limiting the performance of physical implementations of quantum protocols is the noise registered by the measurement systems. While there can be several types of noise, depending on the setup configuration, most of them (*e.g.* dark counts, stray light, Raman scattering induced by other signals propagating through the same fiber) are totally uncorrelated with the real signals. This means that typically most of the noise is registered by the detectors at random times. Thus, it can be filtered out by defining narrow detection windows centered at the expected arrival times of the signal photons to the detection systems, and accepting only measurement results obtained inside those windows. This procedure, called temporal filtering, can be seen as one of the most effective ways to reduce the noise plaguing the realistic implementations of quantum protocols [25].

Unfortunately, the duration time of a single detection window cannot be made infinitely small. The most basic limitation for this quantity stems from the detector timing jitter, which is non-zero for all types of realistic devices. However, if the wavelength of photons emitted from a given source is characterized by a probability distribution function and the channel utilized for their transmission to the measurement system is dispersive, it may happen that the temporal width of those photons at their arrival to the detector would be much larger than the jitter. The temporal broadening effect, described above, would then force the experimenter to define longer detection windows for the measurement system, because otherwise considerable amount of real signals would have

\* miklas@fizyka.umk.pl

been lost. In consequence, it is the major factor limiting the effectiveness of the temporal filtering method for long-distance QC schemes with SPDC sources.

Taking into account the above consideration, it is now clear that the minimization of the temporal width of the emitted photons after their propagation through telecommunication fibers is very important. However, to the best of our knowledge such a general optimization has not yet been done. Only recently it was shown that changing the properties of pairs of photons can indeed significantly influence the performance of quantum protocols [26–28]. In Ref. [28] preliminary optimization of SPDC source for a specific setup configuration was also performed.

In this manuscript we generalize the optimization of photon pairs characteristics for an arbitrary QC scheme. We also investigate the influence of non-zero timing jitter of realistic detectors on the obtained results and discuss whether the theoretically optimal values can be implemented in practice. Finally, we estimate the advantage stemming from the optimization of SPDC source on the maximal security distance of a basic quantum key distribution scheme. Our paper is organized as follows. First, in Sec. II, we derive analytical formulas for temporal widths of a heralded and non-heralded photon emitted from SPDC source and propagated through dispersive medium. The general optimization of the source parameters, minimizing those widths, is done in Sec. II A. Next, in Sec. II B we examine the counterintuitive effect of the reduction of temporal width of a SPDC photon by adding dispersion to the quantum channel through which the other photon from the pair travels. We show that such an effect can be seen not only when the photon pair emission time is not known, as previously suggested in [27], but also in more general case. In Sec. II C we investigate the influence of non-zero detection timing jitter on the measured temporal width of SPDC photons. The achievability of the theoretically optimal setup parameters for realistic SPDC sources is considered in Sec. II D. In this part of our manuscript we derive the formula for the effective phase-matching function width for a source based on BBO crystal, cut for type I SPDC process generating a pair of 1550 nm photons. We then calculate this parameter for different lengths and orientations of the crystal and compare the results with the optimal value of the effective phase-matching function width derived from our source optimization strategy. Finally, in Sec. III, we apply this strategy to a basic quantum key distribution (QKD) scheme. We demonstrate that full optimization of a SPDC source can be used to increase the maximal security distance of such scheme by as much as 50%, which corresponds to several tens of kilometers for each arm of the setup. The paper is summarized in Sec. IV.

## II. TEMPORAL WIDTHS OF SPDC PHOTONS

We consider SPDC source of photon pairs based on a nonlinear crystal parametrized by the effective phase-

matching function width  $\sigma$ , pumped by laser pulses of temporal width  $\tau_p$ . The former one of these two quantities is a convenient single parameter describing the crystal, which depends on its length, optical axis orientation and the directions of propagation of the pump and output photons [23]. The spectral wavefunction of the pairs of photons produced by such a source can be written in the following form [24, 29]:

$$\phi(\nu_A, \nu_B) = N \exp\left(-\frac{(\nu_A - \nu_B)^2}{\sigma^2} - \frac{(\nu_A + \nu_B)^2 \tau_p^2}{4}\right), \quad (1)$$

where  $\nu_A, \nu_B$  are frequency detunings from the respective central frequencies and  $N$  is the normalization constant. We assume that the pairs of photons generated inside the crystal are subsequently transferred to single-photon detectors through quantum channels of length  $L_A$  and  $L_B$ , characterized by the group velocity dispersion (GVD) equal to  $2\beta_A$  and  $2\beta_B$ , respectively. This scheme is illustrated in Fig.1. In this manuscript we use the notation  $D_X \equiv \beta_X L_X$  (for  $X = A, B$ ) to simplify the subsequent mathematical expressions.

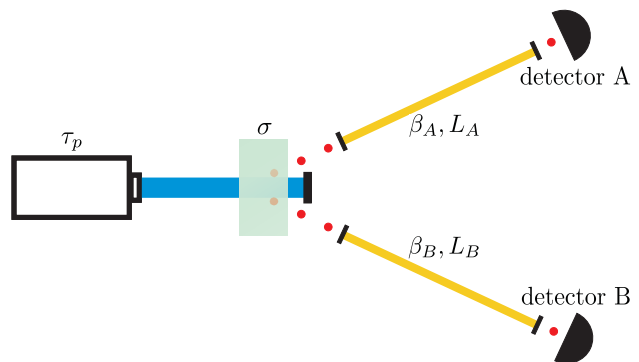


FIG. 1. The generic setup configuration for the detection of SPDC photons. A nonlinear crystal characterized by the effective phase-matching function width  $\sigma$  is pumped by a laser generating pulses of duration  $\tau_p$ .

To calculate the temporal wavefunction of the pair of SPDC photons after their propagation through the dispersive media we utilize the following formula [26]:

$$\psi_{D_A D_B}(t_A, t_B) = \int dt'_A dt'_B S(t_A, t'_A, D_A) S(t_B, t'_B, D_B) \psi(t'_A, t'_B), \quad (2)$$

where

$$S(t_X, t'_X, D_X) = \frac{1}{\sqrt{4\pi i D_X}} \exp\left(\frac{i(t_X - t'_X)^2}{4D_X}\right) \quad (3)$$

is the single-photon propagator and  $\psi(t'_A, t'_B)$  denotes the temporal wavefunction of the photons before their propagation. This wavefunction can be obtained from  $\phi(\nu_A, \nu_B)$ , given by the expression (1), through Fourier transform.

Throughout this work we assume that the information on the time moments at which the source sends pump pulses to the crystal in order to generate subsequent pairs of photons is distributed to the experimenter. Without any loss of generality we focus on calculating the temporal width of the photon entering the detector A (photon A) in Fig. 1. If an experimenter knows nothing about the detection time of the other photon (photon B), the probability distribution function for the detection time of photon A can be calculated as the marginal distribution

$$p_A(t_A) = \int dt_B |\psi_{D_A D_B}(t_A, t_B)|^2. \quad (4)$$

In this case the temporal width of photon A reads:

$$\tau_A = \frac{\sqrt{(\tau_p^2 + D_A^2 \sigma^2)(4 + \sigma^2 \tau_p^2)}}{2\sigma\tau_p} \quad (5)$$

On the other hand, if the detection time of photon B is known to be  $T_B$ , the probability distribution function for the detection time of photon A takes the form of

$$p_{Ah}(t_A, t_B = T_B) = \frac{|\psi_{D_A D_B}(t_A, t_B = T_B)|^2}{\int dt_A |\psi_{D_A D_B}(t_A, t_B = T_B)|^2}. \quad (6)$$

Its temporal width is then given by:

$$\tau_{Ah} = \sqrt{\frac{16(\tau_p^2 - D_A D_B \sigma^2)^2 + (D_A + D_B)^2(\sigma^2 \tau_p^2 + 4)^2}{4(\tau_p^2 + D_B^2 \sigma^2)(\sigma^2 \tau_p^2 + 4)}}. \quad (7)$$

The temporal width of photon B in the non-heralded and heralded case can be obtained immediately from the expressions (5) and (7), respectively, by switching  $D_A$  to  $D_B$  and vice versa.

As was already written in Sec. I, in the context of QC applications it is generally desirable for the temporal functions of SPDC photons to be as narrow as possible in order to allow for effective temporal filtering of various types of noise. Therefore, a natural question is: what are the optimal values of the source parameters,  $\tau_p$  and  $\sigma$ , for which the temporal widths of SPDC photons, calculated above, are the lowest?

### A. Optimization of temporal widths

In practice it is typically much easier to calibrate the temporal width of pump laser pulses than to modify the effective phase-matching function for the nonlinear crystal, since the latter usually requires replacing the crystal itself. Therefore, let us first consider the situation in which the experimenter can only change the pump laser utilized by the SPDC source, while the crystal is fixed. In this case  $\tau_A$  reaches its lowest value, equal to

$$\tau_A^{\text{low}} = \frac{2 + |D_A| \sigma^2}{2\sigma}, \quad (8)$$

for  $\tau_p = \sqrt{2|D_A|}$ , as has been already shown in Ref. [28]. Since  $\tau_A$  does not depend on  $D_B$ , the above result is identical for the symmetric and asymmetric setup configurations. In the symmetric case also  $\tau_{Ah}$  reaches its minimum for  $\tau_p = \sqrt{2|D_A|}$ , which reads:

$$\tau_{Ah}^{\text{low, sym}} = \sqrt{\frac{2|D_A|(D_A^2 \sigma^4 + 4)}{(|D_A| \sigma^2 + 2)^2}}. \quad (9)$$

However, the optimization of  $\tau_{Ah}$  over  $\tau_p$  for the asymmetric setup configuration is much more complicated. In this case the function  $\tau_{Ah}(\tau_p)$  does not always have a global minimum and the conditions for its existence heavily depend on the relationship between  $D_A$ ,  $D_B$  and  $\sigma$ . While these conditions are very complex in the general scenario, they can be considerably simplified if we assume that  $D_A$  and  $D_B$  have the same sign, which is certainly a justified assumption in realistic situations. To write them explicitly we first introduce the following notation:

$$\xi_{i,j} = \left[ i \frac{D_A - D_B + j \sqrt{(D_A - D_B)^2 - 8D_A(D_A + D_B)}}{2D_A D_B} \right]^{1/2}, \quad (10)$$

$$\zeta_{i,j} = \left[ i \frac{D_A - D_B + j \sqrt{(D_A - D_B)^2 - 8D_B(D_A + D_B)}}{D_B(D_A + D_B)} \right]^{1/2}. \quad (11)$$

For the typical QC scheme, in which single-mode fibers (SMFs) are used, it is always  $D_A, D_B < 0$ . In this case the right-hand side of the expression (7) reaches its minimum for

$$\tau_p^{(-)} = 2 \sqrt{-\frac{2(D_A + D_B) - \sigma^2 D_B(D_A - D_B) + \sigma^4 D_A D_B^2}{8 + 2\sigma^2(D_A - D_B) + \sigma^4 D_B(D_A + D_B)}}. \quad (12)$$

in the three following cases: (1) when  $10.7 D_A \approx (4\sqrt{2} + 5)D_A < D_B < [(4\sqrt{2} - 5)/7] D_A \approx 0.094 D_A$ , (2) when  $D_B \leq (4\sqrt{2} + 5)D_A$  and one of the inequalities  $\sigma < \xi_{+1,-1}$  or  $\xi_{+1,+1} < \sigma$  is true, (3) when  $[(4\sqrt{2} - 5)/7] D_A \leq D_B$  and one of the inequalities  $\sigma < \zeta_{-1,+1}$  or  $\zeta_{-1,-1} < \sigma$  is true. If none of the above sets of conditions is fulfilled, then the function  $\tau_{Ah}(\tau_p)$  does not have a global minimum. If  $D_B \leq (4\sqrt{2} + 5)D_A$  but  $\xi_{+1,-1} \leq \sigma \leq \xi_{+1,+1}$  it is monotonically increasing, meaning that the lowest temporal width of photon A is reached for  $\tau_p \rightarrow 0$ . On the other hand if  $[(4\sqrt{2} - 5)/7] D_A \leq D_B$  but  $\zeta_{-1,+1} \leq \sigma \leq \zeta_{-1,-1}$  the function  $\tau_{Ah}(\tau_p)$  always decreases when  $\tau_p$  grows. Therefore, in this situation the lowest temporal width of photon A is reached for  $\tau_p \rightarrow \infty$ .

The examples of how the function  $\tau_{Ah}(\tau_p)$  depends on different values of  $\sigma$  in the cases of symmetric and highly asymmetric setup configurations can be seen in Fig. 2. The plots were made with the assumption that  $\beta_A = \beta_B = -1.15 \times 10^{-26} \text{ s}^2/\text{m}$ , corresponding to typical fiber (SMF28e+), which is the most common type of communication channels used in practical QC schemes.

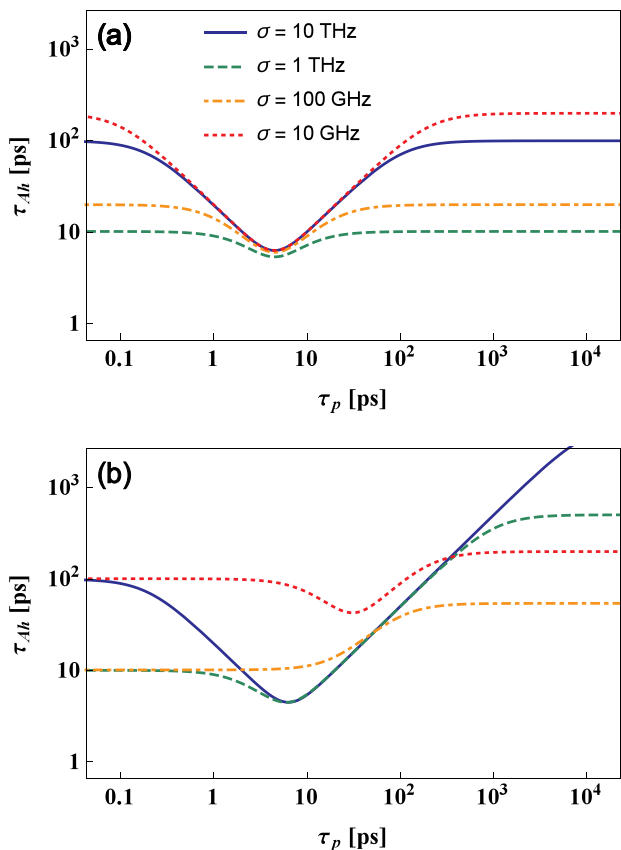


FIG. 2. Temporal width,  $\tau_{Ah}$ , of the heralded photon A plotted as a function of the duration time of a pump laser pulse for the case when two standard SMF fibers of length  $L_A = 1$  km and (a)  $L_B = 1$  km, (b)  $L_B = 100$  km are placed between the crystal and single-photon detectors. The legend corresponds to both panels.

This assumption was also used for drawing all of the other figures shown in this manuscript. As can be seen in Fig. 2 (a) in symmetric case the function  $\tau_{Ah}(\tau_p)$  has a well-defined minimum for any  $\sigma$ . Its value depends on the effective phase-matching function width relatively weakly, while the value of  $\tau_p$  for which this minimum is reached is totally independent of  $\sigma$ . The situation is much different in the highly asymmetric case illustrated in panel (b). Here both the optimal value of  $\tau_p$  and the minimal value of  $\tau_{Ah}$  significantly depend on the effective phase-matching function width. Moreover, for  $\sigma = 100$  GHz (corresponding to 0.13 nm at 1550 nm in terms of wavelength) none of the conditions for the existence of the global minimum of  $\tau_{Ah}$  is fulfilled. In this situation  $\tau_{Ah}(\tau_p)$  is monotonically increasing function (see the orange dot-dashed line). It can also be seen that in the asymmetric scenario the comparison between the functions of  $\tau_{Ah}(\tau_p)$  plotted for different  $\sigma$  heavily depends on  $\tau_p$ . For example, while for very short pump pulses the value of  $\tau_{Ah}$  calculated for  $\sigma = 1$  THz is much smaller than for  $\sigma = 10$  GHz, it is the opposite for large  $\tau_p$ . The situation like this cannot be seen in the symmetric case.

Similar analysis to the one presented above can be performed for  $D_A, D_B > 0$ . This condition represents *e.g.* the scenario in which an experimenter utilizes dispersion compensating fibers (DCFs) instead of typical SMFs. In this case a global minimum exists for the function  $\tau_{Ah}(\tau_p)$  in the three following situations: (1) when  $[(4\sqrt{2} - 5)/7] D_A < D_B < (4\sqrt{2} + 5)D_A$ , (2) when  $D_B \leq [(4\sqrt{2} - 5)/7] D_A$  and at the same time  $\sigma < \zeta_{+1,-1}$  or  $\zeta_{+1,+1} < \sigma$  is true, (3) when  $(4\sqrt{2} + 5)D_A \leq D_B$  and at the same time  $\sigma < \xi_{-1,+1}$  or  $\xi_{-1,-1} < \sigma$  is true. In all of these cases the optimal value of  $\tau_p$  equals

$$\tau_p^{(+)} = 2\sqrt{\frac{2(D_A + D_B) + \sigma^2 D_B(D_A - D_B) + \sigma^4 D_A D_B^2}{8 - 2\sigma^2(D_A - D_B) + \sigma^4 D_B(D_A + D_B)}}. \quad (13)$$

If  $D_B \leq [(4\sqrt{2} - 5)/7] D_A$  but  $\zeta_{+1,-1} \leq \sigma \leq \zeta_{+1,+1}$  the smallest temporal width is reached for  $\tau_p \rightarrow 0$ , while if  $(4\sqrt{2} + 5)D_A \leq D_B$  but  $\xi_{-1,+1} \leq \sigma \leq \xi_{-1,-1}$  the function  $\tau_{Ah}(\tau_p)$  monotonically decreases for  $\tau_p \rightarrow \infty$ .

Contrary to the scenario when the nonlinear crystal is fixed, full optimization of a SPDC source over the parameters  $\tau_p$  and  $\sigma$  cannot be done analytically in the general case. Nevertheless, it can be performed for the symmetric setup configuration, when  $D_A = D_B \equiv D$ . This task has already been done in our previous paper, [26], where it was shown that in the symmetric case the optimal values of the SPDC source parameters are  $\tau_p^{\text{sym}} = \sqrt{2|D|}$  and  $\sigma^{\text{sym}} = \sqrt{2/|D|}$ . For those numbers the function  $\tau_{Ah}$  reaches its absolute minimum, equal to  $\tau_{Ah}^{\text{sym}} = \sqrt{2|D|}$ . In the symmetric case  $\tau_{Ah}$  exhibits high symmetry both as a function of  $\tau_p$  and  $\sigma$ . It can be seen in Fig. 3(a), where the temporal width of the photon A is plotted for  $L_A = L_B = 1$  km. For comparison, in Fig. 3(b) we plot  $\tau_{Ah}$  for the highly asymmetric case of  $L_A = 1$  km and  $L_B = 100$  km.

## B. Dependence on the length of the heralding arm

In the case of asymmetric QC scheme it is possible to reduce the temporal width of SPDC photons propagated through one of its arms by introducing a proper amount of dispersion to the other arm (*e.g.* by adjusting its length). This can have a positive effect on the performance of QC protocols in some setup configurations, as was already shown in Ref. [27] in the context of asymmetric QKD scenario. However, the framework used in Ref. [27] was based on the analysis of spectral correlation and generated photon widths. It gave a general insight into the physical mechanisms yielding the optimal performance of the QC scheme, but must be reformulated to be directly related to the typical experimental scenario. Here we accomplish this goal using the parameters  $\sigma$  and  $\tau_p$ .

In Fig. 4 it can be seen how the temporal width  $\tau_{Ah}$ , optimized over the duration time of the pump laser pulses, changes with different values of  $L_B$  and  $\sigma$ . It is

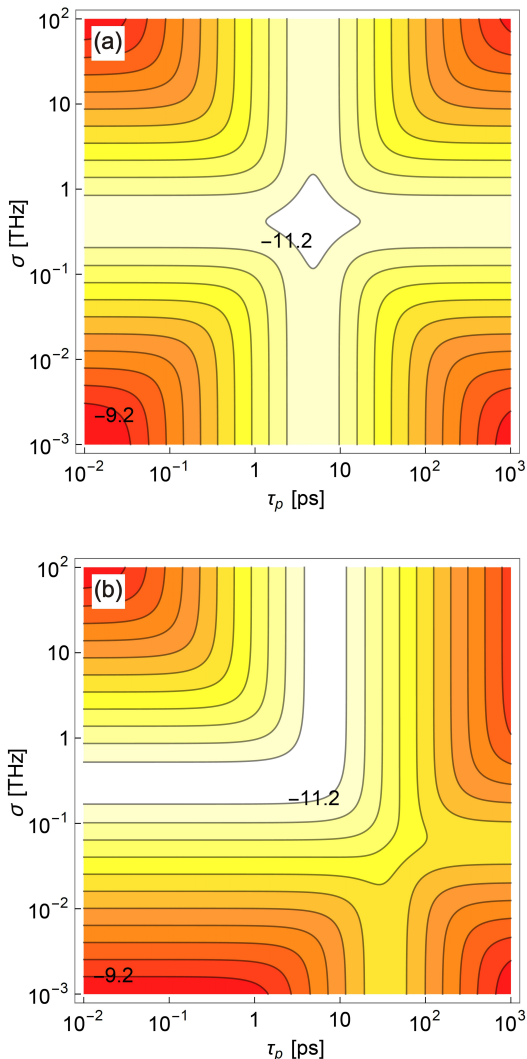


FIG. 3. Logarithm of the temporal width of the heralded photon A,  $\tau_{Ah}$ , at the entrance to the detector, plotted as a function of the duration time of the pump laser pulse,  $\tau_p$ , and the effective phase-matching function width of the nonlinear crystal,  $\sigma$ , for the case when the source is connected with the detectors by SMFs of length  $L_A = 1$  km and (a)  $L_B = 1$  km or (b)  $L_B = 100$  km. The contours shown in both plots represent values from  $\log_{10} \tau_{Ah} = -11.2$  to  $\log_{10} \tau_{Ah} = -9.2$  with constant 0.2 spacing.

interesting to note that if the effective phase-matching function width is significantly larger than its optimal value,  $\sigma_{\text{opt}}$ , extending the length of the heralding arm always leads to the reduction of  $\tau_{Ah}$ . However, this effect is more prominent for smaller distances, while for  $L_B \rightarrow \infty$  the temporal width of the heralded photon asymptotically decreases to a fixed value. On the other hand, when  $\sigma < \sigma_{\text{opt}}$ , extending the heralding arm has the opposite effect on  $\tau_{Ah}$  to the one described above.

Relating the above consideration to the analysis performed in Ref. [27] one can conclude that for  $\sigma > \sigma_{\text{opt}}$  the maximal security distance in one arm of the asymmetric

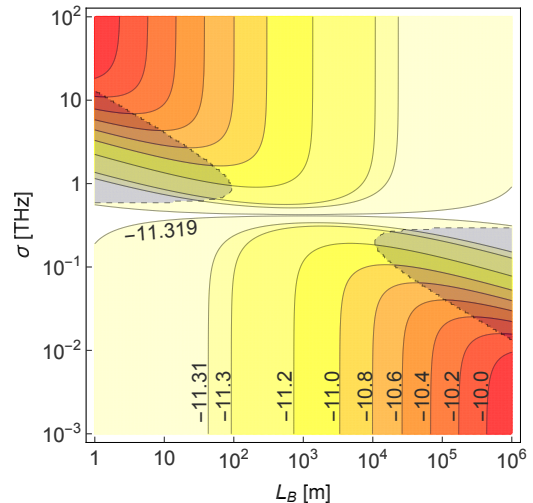


FIG. 4. Logarithm of the temporal width of the heralded photon A at the entrance to the detector,  $\tau_{Ah}$ , shown as a function of the length of the heralding SMF quantum channel,  $L_B$ , and the effective phase-matching function width of the nonlinear crystal,  $\sigma$ , plotted for the case when the source is connected with the detector A by another SMF quantum channel of length  $L_A = 1$  km. For every pair of values  $(L_B, \sigma)$  the calculated temporal width has been optimized over the pump laser pulse duration  $\tau_p$ . The overshadowed area near the left [right] edge of the figure corresponds to the range of  $(L_B, \sigma)$ , for which the optimal value of  $\tau_{Ah}$  is reached for  $\tau_p \rightarrow \infty$  [ $\tau_p \rightarrow 0$ ]. For other combinations of  $L_B$  and  $\sigma$  the optimal value of  $\tau_p$  is given by the formula (12). The spacing between the neighboring contours becomes smaller than 0.2 for  $\log_{10} \tau_{Ah} < -11.2$  in order to better illustrate how this function behaves near its minimum.

QKD scheme can be extended by introducing more dispersion to the other arm. This conclusion is similar to the one stated in Ref. [27]. However, as we have already mentioned before, in this work we assume that the information on the time moments at which the source sends pump pulses to the crystal is known to Alice and Bob. Therefore, the aforementioned security improvement can be seen even when the global time reference is distributed to the legitimate participants of the QKD protocol, contrary to the results of Ref. [27]. Consequently, it can potentially have much broader practical application.

As indicated above, the values of  $\tau_{Ah}$  illustrated in Fig.4 are optimized over the temporal width of pump laser pulses. The regions of  $(L_B, \sigma)$  for which the optimal values of  $\tau_p$  are reached for  $\tau_p \rightarrow \infty$  and for  $\tau_p \rightarrow 0$  correspond to the overshadowed areas near the left and right edges of Fig.4, respectively. On the other hand the region of  $(L_B, \sigma)$  for which the optimal values of  $\tau_p$  are given by the formula (12) is not overshadowed. This picture shows that the conditions for the function  $\tau_{Ah}(\tau_p)$  to have a global minimum, derived in Sec. II A, are always fulfilled when the channel parameters,  $D_A$  and  $D_B$  are of the same order of magnitude. Only for highly asymmetric

schemes this function can be minimized asymptotically for  $\tau_p \rightarrow \infty$  or  $\tau_p \rightarrow 0$ .

### C. Detector timing jitter

It can be seen in Fig.2–Fig.4 that if the SMF connecting the source with the detector A is of the order of 1 km, the temporal width  $\tau_{Ah}$  can be reduced even below the level of 10 ps. This value is comparable with the timing jitter of the best currently existing single-photon detectors [30–33]. Therefore, in this subsection we carefully analyze the influence of non-zero timing jitter on the presented method.

Non-zero timing jitter generally means that the detection time of photon A,  $t_A$ , is different from the time of its arrival at the measurement system,  $t_A^0$ . The difference between these two quantities can be described by the probability distribution function of the Gaussian form

$$q(t_A, t_A^0, \tau_{JA}) = M_A \exp\left(-\frac{(t_A - t_A^0)^2}{2\tau_{JA}^2}\right), \quad (14)$$

where  $\tau_{JA}$  is the value of the jitter and  $M_A$  is the nor-

malization constant. Then, the probability distribution for the detection time of this photon in the case when the detection time of photon B is unknown can be calculated as

$$\pi_A(t_A) = \int dt_A^0 p_A(t_A^0) q(t_A, t_A^0, \tau_{JA}), \quad (15)$$

where the function  $p_A(t_A^0)$  is given by the formula (4). It is straightforward to check that the standard deviation of  $\pi_A(t_A)$  is equal to

$$\tau_A^J = \sqrt{\tau_{JA}^2 + \tau_{JA}^2}. \quad (16)$$

The above formula gives the temporal width of the non-heralded photon A for the case of non-zero jitter.

While the value of  $\tau_A^J$  depends only on the timing jitter of the detector A, the analogous temporal width of photon A found in the heralded case,  $\tau_{Ah}^J$ , would obviously be influenced also by the timing jitter of the other detector,  $\tau_{JB}$ . In order to calculate it one has to take the joint probability formula for the detection of photon A at the time  $t_A$  and the detection of photon B at the time  $t_B$ , which can be derived from (2) as  $p_{AB}(t_A, t_B) = |\psi_{D_A D_B}(t_A, t_B)|^2$ , and modify it to the following form:

$$\pi_{AB}(t_A, t_B) = \int dt_A^0 \int dt_B^0 p_{AB}(t_A^0, t_B^0) q(t_A, t_A^0, \tau_{JA}) q(t_B, t_B^0, \tau_{JB}), \quad (17)$$

where  $t_B^0$  is the arrival time of photon B to the heralding detector. The probability distribution of the detection time of photon A, conditioned on the detection of photon B at the time  $T_B$ , is then given by

$$\pi_{Ah}(t_A, t_B = T_B) = \frac{\pi_{AB}(t_A, t_B = T_B)}{\int dt_A \pi_{AB}(t_A, t_B = T_B)}. \quad (18)$$

The standard deviation of the resulting function is

$$\tau_{Ah}^J = \sqrt{\tau_{Ah}^2 + \tau_{JA}^2 + X\tau_{JB}^2}, \quad (19)$$

where  $\tau_{Ah}$  is the temporal width of the photon A calculated for zero jitter case and

$$X = \frac{(\tau_p^2 - D_A D_B \sigma^2)^2 (\sigma^2 \tau_p^2 - 4)^2}{(\tau_p^2 + D_B^2 \sigma^2)^2 (\sigma^2 \tau_p^2 + 4)^2}. \quad (20)$$

In order to estimate the range of fiber lengths for which the detection jitter can have significant influence on the temporal widths of SPDC photons we consider the situation in which these widths would be the smallest in the zero-jitter case. Therefore, in Fig. 5 we compare the temporal widths of the heralded photon A,  $\tau_{Ah}^J$ , optimized over the source parameters,  $\sigma$  and  $\tau_p$ , calculated

as a function of the propagation distance for a few different values of  $\tau_{JA}$  and  $\tau_{JB}$ . The plots are made for the symmetric QC scheme. As one can see there, if  $L_A$  and  $L_B$  are shorter than a few kilometers, the jitter significantly influences  $\tau_{Ah}^J$  even if it is much smaller than in the case of the state-of-the-art single-photon detectors. Therefore, to exploit the full potential of the optimization method presented in this paper further development of photon detection technology will be needed. At present, however, it is certainly possible to make the influence of detection jitter negligible if the propagation distance is of the order of tens of kilometers or more. To conclude, the results of our investigation, presented in Fig. 5, indicate that if the experimenter wants to fully optimize the short-distance QC scheme, the detection jitter of realistic single-photon detectors can become one of the most important factors. On the other hand, for long-distance communication schemes the jitter can be safely neglected.

### D. Realistic effective phase-matching function width

In principle, in the case of any specific QC setup configuration, the optimization of a SPDC source according

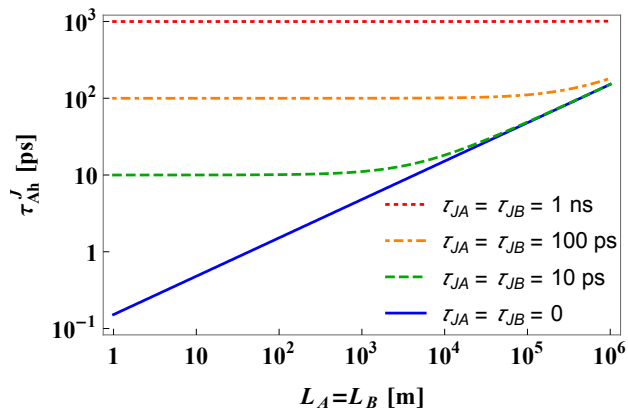


FIG. 5. Temporal width,  $\tau_{Ah}^j$ , of the heralded photon, optimized over the SPDC source parameters  $\sigma$  and  $\tau_p$ , plotted as a function of the length of SMFs separating the source and the photon detection systems in the case of symmetric setup configuration. The detectors' timing jitter is defined as the standard deviation of the detection time probability function.

to the rules presented in Sec. II A allows the experimenter to easily find the most favourable values of a pump laser pulse duration and an effective phase-matching function width. However, one may wonder if these theoretically optimal values would be achievable for realistic SPDC sources. It is much easier to answer this question in the context of the pump laser pulse duration, owing to the variety of commercially available lasers, ranging from the CW to femtosecond ones. According to the results of Sec. II A, the optimal value of  $\tau_p$  generally grows with the propagation distance and already for  $L_A = L_B = 1$  m it is approximately equal to 150 fs. Therefore, one can safely say that the theoretically optimal pump laser pulse duration should be achievable for basically every realistic QC scheme.

Performing similar analysis in the context of effective phase-matching function width associated with different kinds of nonlinear crystals is much more complexed. The value of  $\sigma$  depends not only on the type of nonlinear material, but also on several other parameters such as the crystal length or its optical axis orientation [24]. However, in order to get some intuition in this matter, we analyzed here a specific case of BBO crystal cut for degenerate type I SPDC process, in which 775 nm pump photons are converted to pairs of 1550 nm photons. In this situation the value of  $\sigma$  can be derived by utilizing the formula (2) from Ref. [24]. The specific parameters of BBO crystal, needed for this calculation, can be found in Ref. [34]. The results of our investigation are presented in Fig. 6, where the effective phase-matching function width was plotted as a function of the angle  $\alpha$  between the central propagation directions of the pump photons and the SPDC photons. The calculations were made for several different values of the crystal length,  $L_{\text{cryst}}$ , and the width of transverse spatial mode collected by the SMFs,  $W_f$ . Additionally, the optimal values of  $\sigma$  for symmetric

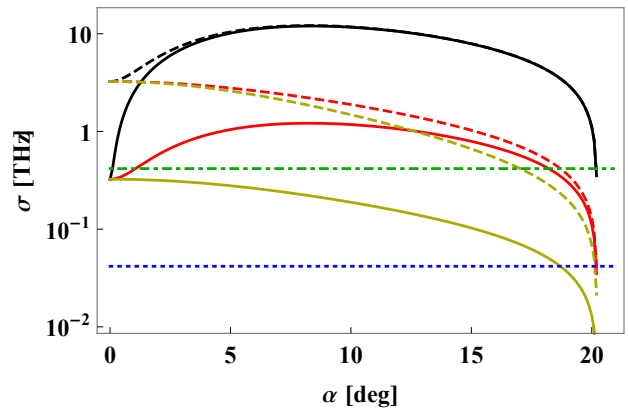


FIG. 6. Effective phase-matching function width,  $\sigma$ , calculated for BBO crystal cut for 750 nm  $\rightarrow$  1550 nm + 1550 nm type I SPDC process, plotted as a function of the angle  $\alpha$  between the central propagation directions for the pump photons and the generated photons. The plots are made for the crystal length equal to  $L_{\text{cryst}} = 1$  cm (solid lines) and  $L_{\text{cryst}} = 1$  mm (dashed lines), and for the following widths of the transverse spatial modes collected by the SMFs,  $W_f$ : 10  $\mu\text{m}$  (black lines), 100  $\mu\text{m}$  (red lines), 1 mm (yellow lines). Blue dotted (green dot-dashed) line correspond to the optimal value of  $\sigma$ , calculated for the symmetric QC setup with SMF quantum channels of 100 km (1 km) length.

QC setup configuration using SMFs of length  $L = 1$  km and  $L = 100$  km were marked in this figure for comparison.

The most important conclusion that can be drawn from Fig. 6 is that for the example source based on BBO crystal analyzed here the theoretically optimal values of the effective phase-matching function width can be very difficult to obtain in most practical situations. This goal seems to be especially hard to achieve for the case of collinear source configuration, *i.e.* when  $\alpha = 0$ , which is often the most convenient one in practice. In this situation, even when using exceptionally long BBO crystals, one may hope to obtain  $\sigma^{\text{opt}}$  width only for short-distance QC schemes. In principle, smaller widths of the effective phase-matching function can be get when the values of  $W_f$  are sufficiently large and the BBO crystal is cut to emit pairs of photons at broad angle from the direction of propagation of the pump laser pulses. However, this kind of SPDC source would be significantly more difficult to construct. Moreover, its pair production efficiency and heralding efficiency would most likely be much smaller than for the case of collinear configuration. This would negatively affect the performance of many QC protocols [23].

### III. AN EXAMPLE OF APPLICATION: QUANTUM KEY DISTRIBUTION

To show the potential to improve the performance of QC schemes by optimizing the SPDC source of photon

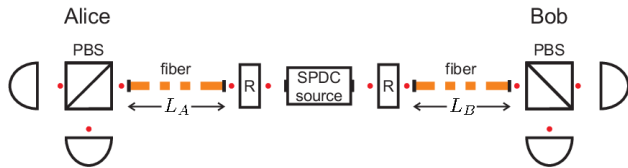


FIG. 7. A simple scheme of discrete-variable QKD with the source of entangled photon pairs placed outside of Alice's and Bob's laboratories. R denotes polarization rotators.

pairs according to the guidance presented in Sec. II A we considered a typical setup configuration for the realization of BB84 protocol in the entanglement-based variant, illustrated in Fig. 7. When calculating the lower bound for the key generation rate that can be obtained from this scheme we assumed that the quantum channels are characterized by the attenuation coefficient  $\alpha_A = \alpha_B = 0.2$  dB/km, which is typical value for 1550 nm photons propagating in SMFs. Furthermore, to simplify the calculations we considered the situation in which the dark counts are the only source of errors in the raw key. Since narrowing the detection windows reduces all the possible errors that are uncorrelated with the real signals in exactly the same way, adding such errors to the model can be easily made just by appropriate increase of the values of  $d_A$  and  $d_B$ . On the other hand, the errors that are connected to the real signals, such as the polarization rotation, would only slightly change the obtained results and not in qualitative way. We also assumed that the SPDC source is perfect, always emitting a single pair of photons when the pump pulse propagates through the crystal. More details of the security analysis can be found in the Appendix.

### A. Symmetric configuration

The potential of the presented method for the optimization of a SPDC source for its use in QC applications can be seen in Fig. 8, where we plotted the lower bound for the key generation rate that can be obtained from the realization of BB84 protocol in the symmetric version of the setup configuration schematically illustrated in Fig. 7. We analyse the cases of (i) non-optimized source with typical value of the effective phase-matching function width and relatively short pump laser pulses, (ii) the source with the same  $\sigma$ , but optimized over the value of  $\tau_p$  and (iii) the fully optimized SPDC source. It can be seen in Fig. 8 that in principle by fully optimizing the source the maximal security distance for the analyzed scheme can be extended by almost one hundred kilometers, which is around 50%, for each of the two existing quantum channels.

Moreover, even partial optimization of the source, just over the pump laser pulse duration, can provide the legitimate participants of the BB84 protocol with about 35–40% of additional security distance for each quantum

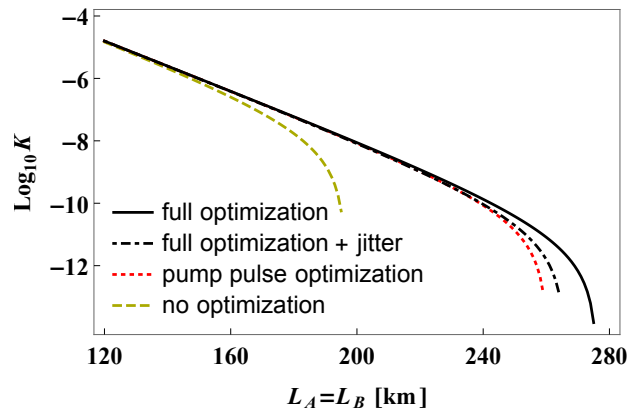


FIG. 8. The lower bound for the key generation rate,  $K$ , plotted as a function of the SMFs length,  $L_A = L_B$ , for BB84 protocol performed in the symmetric version of QKD scheme presented in Fig. 7. The plots are calculated for the following values of the source parameters:  $\sigma = 1$  THz and  $\tau_p = 0.1$  ps (dashed yellow line),  $\sigma = 1$  THz and  $\tau_p = \sqrt{2|\beta|L}$  (dotted red line),  $\sigma = \sqrt{2/(|\beta|L)}$  and  $\tau_p = \sqrt{2|\beta|L}$  (solid black line). The three aforementioned curves are drawn assuming ideal single-photon detectors with no timing jitter. Additionally, dot-dashed black line illustrates the lower bound for the key generation rate calculated in the case when the jitter of all the detectors utilized by Alice and Bob is 100 ps, while the source parameters are  $\sigma = \sqrt{2/(|\beta|L)}$  and  $\tau_p = \sqrt{2|\beta|L}$ .

channel. This result can be seen as especially important in the context of our consideration presented in Sec. II D, which call into question the possibility to fully optimize SPDC sources for long-distance QC in practice. Here we show that even if this task indeed turns out to be impossible, the security of QC schemes can still be significantly improved just by proper optimization of the pump laser.

It is also important to notice, that the results plotted in Fig. 8 do not change considerably if we assume that Alice and Bob use single-photon detectors characterized by detection timing jitter of  $\tau_{JA} = \tau_{JB} = 100$  ps, which is well above the best achievable value for the modern measurement devices [30–32]. In this situation the maximal security distance is shortened only by a few kilometers comparing to the case with ideal single-photon detectors. This result is consistent with the analysis presented in Sec. II C, where it was shown that for very long distances between the SPDC source and the measurement systems only relatively high jitter can significantly influence the temporal width of photons entering the detectors.

### B. Asymmetric configuration

The results shown in Fig. 8 were obtained for the security analysis of the symmetric version of the QKD setup. In Fig. 9 we present the results concerning more general situation, in which the two SMFs connecting the SPDC source with Alice and Bob are not of the same length.



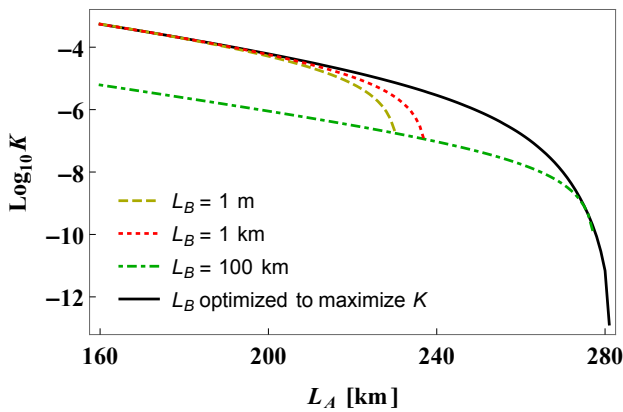


FIG. 9. Lower bound for the key generation rate that can be obtained from the realization of BB84 protocol using the QKD scheme pictured in Fig. 7, plotted as a function of the length  $L_A$  of the SMF used to connect the SPDC source with the laboratory of Alice. All of the plots are made for  $\sigma = 1$  THz, while the values of  $\tau_p$  are numerically optimized.

In this part of our work we specifically focus on checking how changing the length of Bob's fiber can influence the maximal security distance between the source and Alice. This investigation is motivated by the possibility of decreasing the temporal width of the heralded SPDC photon by extending the distance between the source and the heralding detector, discussed in Sec. II B. While such possibility is available only when  $\sigma > \sigma^{\text{opt}}$  (see Fig. 4 (a)), the results of Sec. II D strongly suggests that this requirement can be fulfilled in most practical situations. As can be seen in Fig. 9, the maximal security distance between the source and Alice can be increased by several tens of kilometers just by optimizing the value of  $L_B$  for any given  $L_A$ , instead of fixing it on some short level. As it has already been indicated in Sec. II B, this method works in the situation when both Alice and Bob are provided with the global time reference distributed by the source, which is considerably more practical as compared to Ref. [27].

The method for improving the QKD security presented in this paper is based on the reduction of the amount of noise registered by single-photon detectors during the protocol. Therefore, its effectiveness would be significantly smaller if the decrease of the key generation rate to zero at the maximal security distance was mainly caused by some other factors than the reduction of signal-to-noise ratio below the critical level. Specifically, in more realistic situation than the one considered in this manuscript the QKD security limit could be highly dependent on the probability for producing more than one pair of photons by the utilized SPDC source. However, this probability can be currently made very low [9–11]. Moreover, the damaging influence of the multipair generation events on QKD security can be efficiently reduced by using decoy-pulse method [35–37], which greatly limits the possibility to attack multiphoton pulses by a poten-

tial eavesdropper. Therefore, the noise registered by the measurement systems during the key generation procedure appears to be much bigger obstacle for long-distance QC than the aforementioned imperfection of photon pair sources.

#### IV. SUMMARY AND OUTLOOK

In this work we performed theoretical optimization of SPDC photon pairs for QC schemes with two dispersive quantum channels of arbitrary lengths. It was done over the pump laser pulse duration and the effective phase-matching function width of nonlinear crystal. We derived an analytical formula for the best setting of the pump laser for a given crystal in the most general case. Moreover, we performed full numerical optimization of a SPDC source, demonstrating the possibility to further refine the performance of quantum protocols. We also showed that the temporal width of a SPDC photon can be minimized in one of two possible ways, depending on the exact value of the effective phase-matching function width: either by increasing the dispersion in the quantum channel, *e.g.* by extending the length of the telecommunication fiber, or by decreasing it. The first (second) of these possibilities is available when the effective phase-matching function width is larger (smaller) than its optimal value.

To compare theoretical predictions of our work with capabilities of realistic SPDC sources we investigated the source based on BBO crystal, designed for type I SPDC process generating pairs of 1550 nm photons. For such source we performed analytical estimation of the effective phase-matching function width. It should be noted here that precise calculation of this parameter can be done only numerically and is beyond the scope of this analysis. The obtained results suggests that for most QC schemes the achievable value of the effective phase-matching function width would be significantly larger than the theoretically optimal one. While in some situations the optimal value could be achieved, it would often require relatively large angles between the pump laser pulse direction and the propagation directions of the generated photons. However, such setup configuration would negatively affect the efficiency of SPDC source.

The above consideration raises the question in what situations it would be more beneficial to abandon the full optimization of the SPDC source based on BBO crystal and use the collinear configuration to produce pairs of photons, and when it would be better to push for the full optimization at the expense of efficiency of the source. Further analysis of this problem would be required to reliably answer such question. Moreover, similar investigation performed for other types of nonlinear crystals would be necessary to get the full view on the issue of optimizing SPDC sources for QC applications in practice.

To demonstrate the potential for improving the performance of QC protocols by optimizing SPDC source,

we considered both symmetric and asymmetric QKD schemes. For the symmetric setup configuration the maximal secure communication distance can be increased by several tens of kilometers. The improvement may even reach 50% if only the theoretically optimal value of the effective phase-matching function width is attainable. However, even by properly optimizing only the pump laser it can be possible to increase the maximal security distance by more than 30%. Moreover, we showed that in realistic cases detection timing jitter reduces the maximal security distance by no more than a few kilometers.

Most of the recent record-breaking long-distance realizations of QKD protocols reported in the literature have been implemented using weak coherent pulses and decoy-pulse method [38–41]. However, many papers suggest that heralded single-photon sources could potentially be better for this task [42–46]. This notion can be supported by taking into account the recent advances in the field of heralding efficiency of the SPDC sources [12–15]. However, a serious obstacle for using those devices in fiber-based long-distance communication is the strong temporal broadening of the generated signals. The SPDC source optimization method presented here allows to overcome this important problem.

Since in our work we considered dark counts as the only source of noise, one can expect that this method can provide even better results in more realistic cases. It seems to be especially promising for the QKD performed in commercial fibers populated by strong classical signals, where the level of channel noise caused by those signals is typically very high [47]. Our results can be particularly useful in the case of asymmetric QKD scheme in which the distance between one of the parties and the source is relatively small and the goal is to maximally extend the security length of the quantum channel connecting the source with the other party. A good example of such scenario can be found when considering a communication between a single individual user and a distant node in a multilevel quantum network with several access networks connected to the central backbone [48, 49]. Then, the maximal security distance between two separate access networks could be substantially increased by introducing more dispersion to the quantum channels connecting the individual users with their respective central nodes, as we also demonstrated in this work

## ACKNOWLEDGEMENTS

The authors acknowledge financial support by the Foundation for Polish Science (FNP) (project First Team co-financed by the European Union under the European Regional Development Fund), Ministry of Science and higher Education, Poland (MNiSW) (grant no. 6576/IA/SP/2016) and National Science Centre, Poland (NCN) (Sonata 12 grant no. 2016/23/D/ST2/02064). We wish to thank National

Laboratory of Atomic, Molecular and Optical Physics, Torun, Poland for the support.

## Appendix

In this appendix we briefly discuss the details of the QKD security analysis, the results of which were presented in Sec. III. For the BB84 protocol realized with the perfect SPDC source in the setup configuration illustrated in Fig. 7 the lower bound on the key generation rate  $K$  is given by [50, 51]:

$$K = p_{\text{exp}} [1 - 2H(Q)], \quad (\text{A.1})$$

where  $H(x) = -x \log_2 x - (1-x) \log_2 (1-x)$  is the Shannon entropy and  $Q$  denotes the quantum bit error rate (QBER) in the raw key generated by the legitimate participants of the protocol. In the above formula  $p_{\text{exp}}$  is the probability of accepting a given event by Alice and Bob for the process of key generation. We assume here that the only accepted events are the ones when after the generation of a single SPDC pair of photons both parties get a click at least in one of their detectors.

Obviously, both  $Q$  and  $p_{\text{exp}}$  depend on the duration time of the detection windows chosen by the participants of the protocol. For a single such window of width  $\xi\tau_X$  the probability for registering a photon of temporal width  $\tau_X$  is given by

$$\eta(\xi) = (2\pi)^{-1/2} \int_{-\xi/2}^{\xi/2} dy \exp(-y^2/2) = \text{erf}(\xi/2\sqrt{2}). \quad (\text{A.2})$$

On the other hand, the probability for registering a dark count in one of the two single-photon detectors can be calculated as

$$P_X(\xi) = 2d\xi\tau_X, \quad (\text{A.3})$$

where  $d$  is the dark count rate for a given single-photon detector. For the calculations performed in this work we assumed that  $d = 1$  kHz both in the case of Alice's and Bob's detectors.

In general, choosing the optimal value of  $\xi$  for a given QKD application is not a trivial task. While for short distances between the source and the participants of the protocol it is beneficial to define relatively long detection windows in order to maximize the key rate, when the lengths of quantum channels are close to the maximal security distance it can be better to choose very small  $\xi$  in order to maximally suppress the number of errors detected by Alice and Bob, even at the expense of losing considerable amount of real signals [27]. Therefore, during the calculations performed in this work for every possible pair of values of  $L_A$  and  $L_B$  we optimized the parameters  $\xi_A$  and  $\xi_B$  (describing the relationship between the temporal widths of photons reaching the measurement systems of Alice and Bob, respectively, with

the duration time of the detection windows chosen by them).

The probability  $p_{\text{exp}}$  for the scheme illustrated in Fig. 7 can be approximated by

$$\begin{aligned}
p_{\text{exp}} \approx & T_A \eta(\xi_A) T_B \eta(\xi_B) + \\
& + T_A \eta(\xi_A) [1 - T_B \eta(\xi_B)] P_{Bh}(\xi_B) + \\
& + [1 - T_A \eta(\xi_A)] T_B \eta(\xi_B) P_{Ah}(\xi_A) + \\
& + [1 - T_A \eta(\xi_A)] [1 - T_B \eta(\xi_B)] P_A(\xi_A) P_{Bh}(\xi_B),
\end{aligned} \tag{A.4}$$

where  $T_A$  ( $T_B$ ) is the transmittance of quantum channel connecting the SPDC source with Alice (Bob), given by  $T_A = 10^{-\alpha_A L_A/10}$  ( $T_B = 10^{-\alpha_B L_B/10}$ ). The probabilities for a dark count to be registered by Alice or Bob in a particular detection window, denoted by  $P_{Ah}$  and  $P_{Bh}$  respectively, can be calculated by inserting the expression (7), and the analogous expression for the temporal width of the heralded photon B, into the formula (A.3). On the other hand, in order to obtain  $P_A$  one should use the equation (5) instead of (7). This probability, appearing only in the last term on the right-hand side of Eq. (A.5), is needed to properly account for the case when neither of the signal photons is detected by the measurement systems of Alice and Bob. In this situation one of the dark counts registered by them has to be treated as a “heralding” click, while the other one is “heralded” by it (obviously, the exact choice does not matter here, as can be confirmed by checking that  $\tau_A \tau_{Bh} \equiv \tau_B \tau_{Ah}$ ). On the other hand, the second and third terms on the right-hand side of Eq. (A.5) correspond to the case when only one of the two photons produced by the source causes a click in one of the measurement systems, but the event is still accepted for the key generation process due to a dark count registered in the other detection system in the appropriately narrowed time window. Finally, the first term on the right-hand side of Eq. (A.5) accounts for the desired situation in which both SPDC photons from a given pair are detected by Alice’s and Bob’s measurement

systems.

In the case of the simplified QKD scheme considered in our work an error in the raw key can be generated only if at least one of the signal photons from a given SPDC pair is lost, but the event is still accepted for key generation. Since dark counts occur in the detectors of Alice and Bob totally randomly, in all of such situations the error probability is 50%. Therefore, QBER can be calculated using the expression

$$Q = \frac{p_{\text{exp}} - T_A \eta(\xi_A) T_B \eta(\xi_B)}{2p_{\text{exp}}}. \tag{A.5}$$

Inserting (A.5) and (A.5) into the formula (A.1) allows to obtain the desired equation for the key generation rate.

As a side note it is worth mentioning here that from the expressions derived in this appendix one can easily obtain the formulas needed for the security analysis of a more popular type of QKD schemes called prepare-and-measure. It can be done just by assuming  $T_A \eta(\xi_A) = 1$ . One can also consider a situation in which Alice and Bob use SPDC source, but place it inside Alice’s laboratory. In this case there may be some losses of photons travelling to Alice’s detection system and also some detection noise, which Eve cannot exploit due to the lack of access. If this is the case, one should utilize modified version of the lower bound for the key generation rate, given by

$$K' = p_{\text{exp}} [1 - H(Q) - H(Q_E)], \tag{A.6}$$

where  $Q_E$  quantifies the ratio of errors which can be exploited by Eve. The relationship between  $Q$  and  $Q_E$  would then be as follows:

$$Q_E = Q - \frac{[1 - T_A \eta(\xi_A)] T_B \eta(\xi_B) P_{Ah}}{2p_{\text{exp}}}. \tag{A.7}$$

- 
- [1] C. H. Bennett and G. Brassard, in *Proceedings of the IEEE International Conference on Computers, Systems, and Signal Processing, Bangalore, India*, Vol. 11 (IEEE, New York, 1984) pp. 175–179.
- [2] A. K. Ekert, *Phys. Rev. Lett.* **67**, 661 (1991).
- [3] M. Hillery, V. Bužek, and A. Berthiaume, *Phys. Rev. A* **59**, 1829 (1999).
- [4] C. H. Bennett, G. Brassard, C. Crépeau, R. Jozsa, A. Peres, and W. K. Wootters, *Phys. Rev. Lett.* **70**, 1895 (1993).
- [5] H.-J. Briegel, W. Dür, J. I. Cirac, and P. Zoller, *Phys. Rev. Lett.* **81**, 5932 (1998).
- [6] C. H. Bennett and S. J. Wiesner, *Phys. Rev. Lett.* **69**, 2881 (1992).
- [7] W. H. Louisell, A. Yariv, and A. E. Siegman, *Phys. Rev.* **124**, 1646 (1961).
- [8] D. C. Burnham and D. L. Weinberg, *Phys. Rev. Lett.* **25**, 84 (1970).
- [9] S. Fasel, O. Alibart, S. Tanzilli, P. Baldi, A. Beveratos, N. Gisin, and H. Zbinden, *New J. Phys.* **6**, 163 (2004).
- [10] T. Zhong, X. Hu, F. N. C. Wong, K. K. Berggren, T. D. Roberts, and P. Battle, *Opt. Lett.* **35**, 1392 (2010).
- [11] M. Bock, A. Lenhard, C. Chunnillall, and C. Becher, *Opt. Express* **24**, 23992 (2016).
- [12] E. Pomarico, B. Sanguinetti, T. Guerreiro, R. Thew, and H. Zbinden, *Opt. Express* **20**, 23846 (2012).
- [13] M. Da Cunha Pereira, F. E. Becerra, B. L. Glebov, J. Fan, S. W. Nam, and A. Migdall, *Opt. Lett.* **38**, 1609 (2013).
- [14] S. Ramelow, A. Mech, M. Giustina, S. Gröblacher, W. Wieczorek, J. Beyer, A. Lita, B. Calkins, T. Gerrits, S. W. Nam, A. Zeilinger, and R. Ursin, *Opt. Express* **21**, 6707 (2013).
- [15] F. Kaneda, K. Garay-Palmett, A. B. U’Ren, and P. G. Kwiat, *Opt. Express* **24**, 10733 (2016).
- [16] K. Mattle, H. Weinfurter, P. G. Kwiat, and A. Zeilinger,

- Phys. Rev. Lett. **76**, 4656 (1996).
- [17] D. Bouwmeester, J.-W. Pan, K. Mattle, M. Eibl, H. Weinfurter, and A. Zeilinger, Nature (London) **390**, 575 (1997).
- [18] J.-W. Pan, D. Bouwmeester, H. Weinfurter, and A. Zeilinger, Phys. Rev. Lett. **80**, 3891 (1998).
- [19] T. Jennewein, C. Simon, G. Weihs, H. Weinfurter, and A. Zeilinger, Phys. Rev. Lett. **84**, 4729 (2000).
- [20] D. S. Naik, C. G. Peterson, A. G. White, A. J. Berglund, and P. G. Kwiat, Phys. Rev. Lett. **84**, 4733 (2000).
- [21] W. Tittel, J. Brendel, H. Zbinden, and N. Gisin, Phys. Rev. Lett. **84**, 4737 (2000).
- [22] W. Tittel, H. Zbinden, and N. Gisin, Phys. Rev. A **63**, 042301 (2001).
- [23] P. Kolenderski, W. Wasilewski, and K. Banaszek, Phys. Rev. A **80**, 013811 (2009).
- [24] A. Gajewski and P. Kolenderski, Phys. Rev. A **94**, 013838 (2016).
- [25] K. A. Patel, J. F. Dynes, I. Choi, A. W. Sharpe, A. R. Dixon, Z. L. Yuan, R. V. Penty, and A. J. Shields, Phys. Rev. X **2**, 041010 (2012).
- [26] K. Sedziak, M. Lasota, and P. Kolenderski, Optica **4**, 84 (2017).
- [27] M. Lasota and P. Kolenderski, Phys. Rev. A **98**, 062310 (2018).
- [28] K. Sedziak-Kacprowicz, M. Lasota, and P. Kolenderski, Sci. Rep. **9**, 3111 (2019).
- [29] T. Lutz, P. Kolenderski, and T. Jennewein, Opt. Lett. **39**, 1481 (2014).
- [30] V. Shcheslavskiy, P. Morozov, A. Divochiy, Y. Vakhtomin, K. Smirnov, and W. Becker, Rev. Sci. Instrum. **87**, 053117 (2016).
- [31] Z. Yan, D. R. Hamel, A. K. Heinrichs, X. Jiang, M. A. Itzler, and T. Jennewein, Rev. Sci. Instrum. **83**, 073105 (2012).
- [32] A. Tosi, A. Dalla Mora, F. Zappa, S. Cova, M. A. Itzler, and X. Jiang, in *Society of Photo-Optical Instrumentation Engineers (SPIE) Conference Series*, Vol. 7222 (Proc. of SPIE, 2009) p. 72221G.
- [33] A. Divochiy, M. Misiąszek, Y. Vakhtomin, P. Morozov, K. Smirnov, P. Zolotov, and P. Kolenderski, Opt. Lett. **43**, 6085 (2018).
- [34] V. G. Dmitriev, G. G. Gurzadyan, and D. N. Nikogosyan, *Handbook of Nonlinear Optical Crystals*, 3rd ed. (Springer, 1999).
- [35] W.-Y. Hwang, Phys. Rev. Lett. **91**, 057901 (2003).
- [36] X.-B. Wang, Phys. Rev. Lett. **94**, 230503 (2005).
- [37] H.-K. Lo, X. Ma, and K. Chen, Phys. Rev. Lett. **94**, 230504 (2005).
- [38] Q. H. Liu, X. P. Rong, and D. M. Xun, (2010), 1001.5163.
- [39] B. Korzh, C. C. W. Lim, R. Houlmann, N. Gisin, M. J. Li, D. Nolan, B. Sanguinetti, R. Thew, and H. Zbinden, Nature Photonics **9**, 163 (2015).
- [40] H.-L. Yin, T.-Y. Chen, Z.-W. Yu, H. Liu, L.-X. You, Y.-H. Zhou, S.-J. Chen, Y. Mao, M.-Q. Huang, W.-J. Zhang, H. Chen, M. J. Li, D. Nolan, F. Zhou, X. Jiang, Z. Wang, Q. Zhang, X.-B. Wang, and J.-W. Pan, Opt. Express **117**, 190501 (2016).
- [41] A. Boaron, G. Boso, D. Rusca, C. Vulliez, C. Autebert, M. Caloz, M. Perrenoud, G. Gras, M.-J. L. F. Bussi eres, D. Nolan, A. Martin, and H. Zbinden, Phys. Rev. Lett. **121**, 190502 (2018).
- [42] Q. Wang, X.-B. Wang, and G.-C. Guo, Phys. Rev. A **75**, 012312 (2007).
- [43] Q. Wang and X.-B. Wang, Phys. Rev. A **88**, 052332 (2013).
- [44] J.-R. Zhu, J. Li, C.-M. Zhang, and Q. Wang, Quantum Inf. Process. **16**, 238 (2017).
- [45] X.-Y. Zhou, C.-H. Zhang, C.-M. Zhang, and Q. Wang, Phys. Rev. A **96**, 052337 (2017).
- [46] C.-H. Zhang, C.-M. Zhang, G.-C. Guo, and Q. Wang, Opt. Express **26**, 4219 (2018).
- [47] P. Eraerds, N. Walenta, M. Legre, N. Gisin, and H. Zbinden, N. J. Phys. **12**, 063027 (2010), 0912.1798.
- [48] D. Elkouss, J. Mart inez-Mateo, A. Ciurana, and V. Mart ın, IEEE J. Opt. Commun. Netw. **5**, 316 (2013).
- [49] A. Ciurana, J. Mart inez-Mateo, M. Peev, A. Poppe, N. Walenta, H. Zbinden, and V. Mart ın, Opt. Express **22**, 1576 (2014).
- [50] B. Kraus, N. Gisin, and R. Renner, Phys. Rev. Lett. **95**, 080501 (2005).
- [51] V. Scarani, H. Bechmann-Pasquinucci, N. J. Cerf, M. Du sek, N. L utkenhaus, and M. Peev, Rev. Mod. Phys. **81**, 1301 (2009).